

Crystal chemistry of Cr-spinels from the lherzolite mantle peridotite of Ronda (Spain)

DAVIDE LENAZ,^{1,*} ANGELO DE MIN,¹ GIORGIO GARUTI,² FEDERICA ZACCARINI,²
AND FRANCESCO PRINCIVALLE¹

¹Department of Geosciences, University of Trieste, Via Weiss 8, 34127 Trieste, Italy

²Department of Applied Geosciences and Geophysics, University of Leoben, Peter Tunner Strasse 5, 8700 Leoben, Austria

ABSTRACT

The crystal chemistry of some Cr-spinels from the lherzolite body of the Ronda peridotite in southern Spain has been investigated. Cell edge spans between 8.1692(2) and 8.2367(1) Å, while the oxygen positional parameter u ranges between 0.26306(7) and 0.26351(7). By using the Princivalle thermometer (1999), an intracrystalline closure temperature between 640 and 840 °C has been calculated. The higher temperatures are very close to the intercrystalline temperatures based on the olivine-spinel thermometer calculated by Woodland et al. (2006) for the Ronda orogenic lherzolites suggesting that the intracrystalline closure occurred soon after the intercrystalline closure. By comparison with Cr-spinels from lherzolite mantle xenoliths, it should be noted that: (1) the oxygen positional parameter can be linearly related to the intracrystalline temperature for both mantle peridotite and mantle xenolith Cr-spinels; (2) the intracrystalline closure temperature is reached faster and is higher in Cr-spinels in mantle xenoliths; and (3) Cr content is linearly related to u in mantle peridotite, but not in mantle xenoliths, suggesting the u value in Cr-spinels from mantle peridotite is driven solely by the chemistry of the spinels.

Keywords: Cr-spinel, crystal chemistry, intracrystalline closure temperature, mantle peridotite, Ronda (Spain)

INTRODUCTION

Cr-bearing spinels are widely considered as important petrogenetic indicators due to general relations between spinel chemistry, rock type, and processes, and new understanding has been achieved on igneous/metamorphic events from analyses of spinel-bearing assemblages (Irvine 1967; Sack 1982; Dick and Bullen 1984; Sack and Ghiorso 1991; Roeder 1994; Barnes and Roeder 2001). The relationships between chemistry, structural parameters, and genetic behaviors have been considered by several authors, in fact some structural studies have been previously performed on crystal chemistry of Cr-spinels from mantle xenoliths (Della Giusta et al. 1986; Princivalle et al. 1989; Carraro 2003; Uchida et al. 2005; Nédli et al. 2008), ophiolites (Bosi et al. 2004; Quintiliani et al. 2006), komatiites (Lenaz et al. 2004), in the Bushveld and Stillwater layered complexes (Lenaz et al. 2007; Lenaz et al. in review), and as inclusions in diamonds and kimberlites (Lenaz et al. 2009) to better understand genesis and/or oxidation mechanisms. Cr-bearing spinels from Al-bearing augite dikes and the lherzolite body of Balmuccia (Ivrea-Verbano zone) have been described by Basso et al. (1984), Menegazzo et al. (1997), and Princivalle et al. (1989), whereas Lenaz and Princivalle (1996, 2005) studied detrital Cr-spinels to define their possible provenance.

In spinels, the anions form a nearly cubic close-packed array, parallel to (111) planes, and the cations fill one-eighth of the tetrahedral (T) and half of the octahedral (M) interstices available in the framework. The oxygen atom is linked to three octahedral and one tetrahedral cations, lying, respectively, on

opposite sides of the oxygen layer, to form a trigonal pyramid. Movement of the oxygen atom along the cube diagonal [111] causes the oxygen layers in the spinel structure to be slightly puckered. Through the study of the crystal-chemical parameters of the Cr-spinels in lherzolite body of the Ronda peridotites, we will try to understand their equilibration processes including intracrystalline temperatures and compare them with those of Cr-spinels with similar chemistry from lherzolite mantle xenoliths to verify if differences in structural parameter and cooling history are present.

GEOLOGICAL SETTING

The Ronda massif in southern Spain is the largest (ca. 300 km²) of several orogenic peridotite massifs exposed in the Betic (Spain) and Rif (Northern Morocco) mountain belts in the westernmost part of the Alpine orogen. It was tectonically emplaced during early Miocene times in the internal zones of the Betic Cordillera. Several studies have provided comprehensive reviews of the regional setting of the Ronda massif (Van der Wal and Vissers 1993, 1996; Tubia et al. 1997; Platt et al. 2003, 2006; Booth-Rea et al. 2005; Esteban et al. 2007; Precigout et al. 2007).

Platt et al. (2003) suggested that the Ronda peridotite was exhumed during earliest Miocene time from about 66 km depth and that the main period of exhumation lasted 5 Ma, starting at around 25 Ma. It overlies high-grade metamorphic rocks of clearly crustal origin belonging to the Alpujarride complex, and it is separated from these rocks by brittle faults. It is in contact, to the southeast, with the Malaguide Complex, a thick weakly metamorphic to non-metamorphic Palaeozoic basement, and with

* E-mail: lenaz@units.it

Mesozoic carbonates of the Betic Dorsal to north. Flysch and postorogenic sediments are mainly exposed to the south (Fig. 1). The Ronda massif forms a sheet, at least 1–5 km thick and it mainly consists of lherzolites with subordinate harzburgite and mafic-ultramafic layers and dikes. The peculiarity of the Ronda massif is its distinct metamorphic zoning in a somewhat concentric pattern of kilometer-scale domains showing garnet, spinel, and plagioclase peridotite facies, respectively (Fig. 1). This feature is possibly unique among all the investigated orogenic peridotite massifs. The dimension of the exposure precludes an interpretation in terms of an undisturbed mantle sequence, such that the different peridotite facies are related with different stages of equilibration during the tectonic history of the peridotite. According to the mantle diapir model (Obata 1980), the Ronda peridotite zoning is interpreted in terms of an ascending hot, slowly cooling peridotite mass, in which the garnet-bearing peridotites reflect an early-stage cooling of the rim, whereas the plagioclase peridotites developed in the core of the body during a final stage of uplift. This model thus clearly

indicates that the garnet peridotites should be older than the plagioclase peridotites.

The spinel tectonites represent an old lithospheric mantle, isolated from the convective mantle at 1.36 Ga (Reisberg and Lorand 1995). According to different authors (Van der Wal and Bodinier 1996; Garrido and Bodinier 1999; Lenoir et al. 2001), the significant heating produced the textures and plagioclase-bearing assemblages seen in the southern part of the body, together with textural evidence for partial melting and melt percolation. According to these interpretations, one of the most remarkable features of the Ronda massif is the “recrystallization front” that represents the transition from the spinel-tectonite to the coarse granular peridotite domain. The evolution of the Ronda recrystallization front is considered as an example of thermal erosion and partial melting of subcontinental lithospheric mantle above upwelling asthenosphere. Across the front, the strongly foliated spinel tectonites were converted into coarse granular peridotites whereas garnet-bearing pyroxenite veins melted and recrystallized as garnet-free spinel websterites (Garrido and Bodinier 1999). A few hundred meters ahead of the recrystallization-melting front, the presence of a more diffuse and irregular fertilization front recorded by the precipitation of secondary clinopyroxene in the spinel tectonites demonstrates that at least a smooth thermal gradient existed across the Ronda massif during the melting event. Therefore, the development and shape of the recrystallization front was probably thermally controlled.

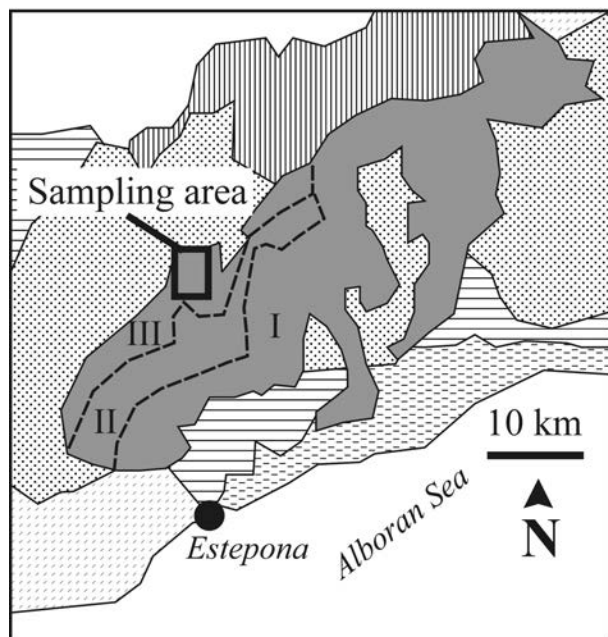
SAMPLING AND PETROGRAPHIC OUTLINES

The collected peridotite samples show different degrees of tectonization and serpentinization even though they are all from the spinel mylonites zone (Fig. 1). Samples 1 and 2 are the least tectonized retaining their original porphyroclastic texture and lherzolitic composition. All the pyroxenes show exsolution lamellae, while olivines are characterized by the presence of kink structures. Both features precede the moment of main fracture. Spinel is pale brown in color and scarcely fractured. Secondary phases fill the fractures representing about 5 and 10% of the thin sections in samples 1 and 2, respectively. Samples 4 and 5 are similar to samples 1 and 2 but with a higher degree of tectonization and fractures filled by serpentine and/or iddingsitic products. A general original porphyroclastic texture is recognizable. Pyroxenes appear often geminate and show evident exsolution lamellae. Olivine is strongly fractured and filled by secondary products. Secondary phases filling the fractures represent about 25% of the thin section. Even in these tectonized samples, spinels are pale brown in color but more fractured than those in samples 1 and 2.

The main features of sample 6 are similar to those of samples 4 and 5. Two different spinels are present. There is a group with allotropic habit very similar to those present in the other samples. The second group, darker in color, shows idiomorphic habit and smaller dimensions compared to the others.

EXPERIMENTAL METHODS

Seven Cr-spinel single crystals were analyzed. X-ray diffraction data were recorded on an automated KUMA-KM4 (K-geometry) diffractometer, using MoK α radiation, monochromatized by a flat graphite crystal, at the University of Trieste (Italy). Twenty-four equivalents of the 12 8 4 reflection, at about 80° of 2 θ , were accurately centered at both sides of 2 θ , and the MoK α peak baricenter



- Mantle peridotite:
 - I = Plagioclase facies
 - II = Spinel facies
 - III = Garnet facies
- ▨ Alpujarride Complex
- ▬ Malaguide Complex
- ▮ Betic Dorsal
- ▧ Allochthonous flysch units
- ▩ Postorogenic sediments

FIGURE 1. Geological sketch map of the Ronda peridotite according to Obata (1980).

was used for cell parameter determination. Data collection was made, according to Della Giusta et al. (1996), up to 55° of θ in the ω - 2θ scan mode, scan width $1.8^\circ 2\theta$, counting time from 20 to 50 s depending on the peak standard uncertainty. Corrections for absorption and background were performed according to North et al. (1968). Structural refinement using the SHELX-97 program (Sheldrick 1997) was carried out against F_o^2 in the $Fd\bar{3}m$ space group (with origin at $\bar{3}m$), since no evidence of different symmetry appeared. Refined parameters were scale factor, oxygen positional parameter (u), tetrahedral and octahedral site occupancies expressed as mean atomic number (m.a.n.), isotropic extinction, and atomic displacement parameters (U). Scattering factors were taken from Prince (2004) and Tokonami (1965). Neutral scattering curves, Mg vs. Fe in T site and Cr vs. Al in M site, were assigned, with the constraints of full site occupancy and equal displacement parameters, and oxygen was considered to be in a partly ionized state (70%). No constraints were imposed by chemical analyses. Crystallographic data are listed in Table 1.

After X-ray data collection, the same crystals used for X-ray data collection were mounted on glass slides, polished and carbon coated for electron microprobe analyses on a CAMECA-CAMEBAX microprobe at IGG-CNR, Padova, operating at 15 kV and 15 nA. A 20 s counting time was used for both peak and total background. Synthetic oxide standards (MgO, FeO, MnO, ZnO, NiO, Al₂O₃, Cr₂O₃, TiO₂, and SiO₂) were used. Raw data were reduced by PAP-type correction software provided by CAMECA. Chemical data are listed in Table 2.

Several different procedures may be adopted to determine cation distribution (Carbonin et al. 1996; Lavina et al. 2002), and very satisfactory results can be obtained by combining data from single-crystal X-ray structural refinements and electron microprobe analyses. This approach simultaneously takes into account both structural and chemical data and reproduces the observed parameters by optimizing cation distributions. Differences between measured and calculated parameters are minimized by a function $F(x)$ taking in consideration different observed quantities such as a_0 , u , T- and M-m.a.n. atomic proportions, and constraints imposed by crystal chemistry (total charges and T and M site populations). Several minimization cycles of $F(x)$ were performed up to convergence. More details about this procedure are described in Carbonin et al. (1996) and Lavina et al. (2002). Cation distributions are listed in Table 2.

RESULTS

Cell edges of the analyzed crystals span from 8.1692(2) to 8.2367(1) Å. In the studied samples, the oxygen positional parameter u is in the range 0.26306(7) to 0.26351(7). The relationships between u and a_0 are reported in Figure 2. In this figure, the values of Cr-spinels from different occurrences such as lherzolite mantle xenoliths (Della Giusta et al. 1986; Princivalle et al. 1989; Carraro 2003; Uchida et al. 2005; Nédli et al. 2008), Al-bearing augite and transitional dikes (sensu Sinigoi et al. 1983) and lherzolite bodies in Balmuccia peridotite complex (Basso et al. 1984; Princivalle et al. 1989; Menegazzo et al. 1997) are also plotted.

TABLE 2. Chemical analyses and cation distribution

Sample	RONDA1	RONDA1A	RONDA2	RONDA4	RONDA5	RONDA6	RONDA6A
MgO	17.5(2)	17.7(3)	17.5(1)	14.6(3)	17.5(3)	13.8(1)	14.2(4)
Al ₂ O ₃	44.2(5)	44.0(4)	44.7(2)	33.9(5)	45.5(3)	28.0(3)	27.7(2)
SiO ₂	0.13(3)	0.12(2)	0.15(2)	0.16(2)	0.19(2)	0.15(2)	0.0
TiO ₂	0.0	0.0	0.05(2)	0.45(2)	0.18(3)	0.06(2)	0.06(2)
Cr ₂ O ₃	25.5(6)	25.5(5)	24.5(3)	32.5(5)	21.5(3)	39.7(5)	39.9(8)
MnO	0.14(6)	0.13(4)	0.16(4)	0.24(6)	0.16(4)	0.24(7)	0.24(6)
FeO _{tot}	12.6(2)	12.3(3)	12.7(4)	17.8(2)	14.3(2)	17.5(1)	16.9(4)
NiO	0.22(8)	0.22(7)	0.21(3)	0.19(7)	0.27(5)	0.0	0.14(2)
Sum	100.3	99.9	99.9	99.9	99.6	99.5	99.0
FeO	12.1(2)	11.8(3)	12.2(4)	15.3(2)	12.3(2)	15.3(1)	14.2(2)
Fe ₂ O ₃	0.52	0.60	0.53	2.81	2.14	2.47	3.00
Sum	100.3	99.99	100.00	100.2	99.8	99.8	99.3
T site							
Mg	0.647	0.649	0.654	0.586	0.644	0.563	0.591
Al	0.070	0.073	0.067	0.047	0.077	0.046	0.048
Si	0.004	0.003	0.004	0.005	0.005	0.004	0.000
Mn	0.003	0.003	0.004	0.006	0.004	0.007	0.006
Fe ²⁺	0.270	0.268	0.266	0.351	0.266	0.379	0.350
Fe ³⁺	0.006	0.004	0.005	0.005	0.005	0.001	0.005
M site							
Mg	0.070	0.072	0.063	0.049	0.072	0.053	0.045
Al	1.362	1.358	1.380	1.114	1.395	0.943	0.934
Ti	0.000	0.000	0.001	0.010	0.004	0.001	0.001
Cr	0.554	0.553	0.532	0.752	0.467	0.949	0.956
Fe ²⁺	0.008	0.003	0.014	0.021	0.017	0.004	0.006
Fe ³⁺	0.002	0.009	0.005	0.050	0.039	0.050	0.055
Ni	0.005	0.005	0.005	0.004	0.006	0.000	0.003
m.a.n. _{x-ray}	48.0(3)	48.0(6)	47.9(6)	52.5(4)	47.9(5)	54.6(3)	54.4(1)
m.a.n. _{chim}	48.2	48.2	48.1	52.4	47.8	54.6	54.4
F(x)	0.168	0.168	0.123	0.134	0.016	0.289	0.204
T (°C)	667	678	644	740	678	842	842

Notes: Mean chemical analyses (10 to 15 spot analyses for each crystal) and cation distribution in T and M site of the analyzed Cr-spinels on the basis of four oxygen atoms per formula unit. Fe³⁺ from stoichiometry. F(x): minimization factor, which takes into account the mean of the square differences between calculated and observed parameters, divided by their square standard deviations. Estimated standard deviations in parentheses.

TABLE 1. Results of structure refinement

Sample	RONDA1	RONDA1A	RONDA2	RONDA4	RONDA5	RONDA6	RONDA6A
a_0	8.1743(1)	8.1692(2)	8.1726(2)	8.2189(4)	8.1710(3)	8.2359(1)	8.2367(1)
u	0.26341(5)	0.26348(8)	0.26351(7)	0.26326(8)	0.26340(7)	0.26310(5)	0.26307(7)
T-O	1.960(1)	1.959(1)	1.961(1)	1.968(1)	1.959(1)	1.970(1)	1.970(1)
M-O	1.940(1)	1.938(1)	1.939(1)	1.952(1)	1.939(1)	1.957(1)	1.958(1)
m.a.n. T	16.0(1)	15.9(1)	16.1(1)	17.1(1)	16.0(1)	17.4(1)	17.0(2)
m.a.n. M	16.0(1)	16.0(2)	15.9(2)	17.7(1)	16.0(2)	18.6(1)	18.2(4)
$U(M)$	0.0039(1)	0.0048(1)	0.0040(1)	0.0045(1)	0.0048(1)	0.0042(1)	0.0039(2)
$U(T)$	0.0059(1)	0.0065(2)	0.0063(2)	0.0063(2)	0.0061(2)	0.0064(1)	0.0060(2)
$U(O)$	0.0059(1)	0.0063(1)	0.0063(2)	0.0066(2)	0.0064(2)	0.0062(1)	0.0067(2)
No. refl.	166	148	146	159	154	165	156
R1	1.90	2.47	2.29	2.28	2.46	1.83	2.09
wR2	3.21	4.47	3.45	4.84	3.31	2.99	3.60
Goof	1.299	1.154	1.255	1.269	1.346	1.324	1.180
Diff. peaks	0.55; -0.72	1.47; -0.92	0.68; -0.83	1.19; -0.89	1.83; -0.99	0.87; -0.44	1.44; -0.87

Notes: a_0 = cell parameter (Å); u = oxygen positional parameter; T-O and M-O = tetrahedral and octahedral bond lengths (Å), respectively; m.a.n. T and M = mean atomic number; $U(M)$, $U(T)$, $U(O)$: displacement parameters for M site, T site, and O; No. refl. = number of unique reflections; R1 all (%), wR2 (%), Goof as defined in Sheldrick (1997). Diff. peaks: maximum and minimum residual electron density ($\pm e/\text{Å}^3$). Space group: $Fd\bar{3}m$. Origin fixed at $\bar{3}m$. $Z = 8$. Reciprocal space range: $-19 \leq h \leq 19$; $0 \leq k \leq 19$; $0 \leq l \leq 19$. Estimated standard deviations in parentheses.

Simple relations between oxygen positional parameter u and cell parameter a_0 allow the calculation of the cation-anion tetrahedral and octahedral bond distances, $T-O \{T-O = a_0 \cdot \sqrt{3} \cdot (1/8 - u^2)\}$ and $M-O \{M-O = a_0 \cdot \sqrt{[(1/2 - u)^2 + 2 \cdot (1/4 - u^2)]}\}$. The T-O and M-O relationships are reported in Figure 3.

With regard to the chemical compositions of the studied Cr-spinels, Cr ranges between 0.467 and 0.956 atoms per formula unit (apfu), Al between 0.982 and 1.472 apfu, Mg between 0.616 and 0.721 apfu, Fe²⁺ between 0.271 and 0.383 apfu, and Fe³⁺ between 0.008 and 0.060 apfu. The compositional range is

related to variable degrees of melt extraction experienced by the individual samples as seen by the linear relationship with Cr content (Fig. 4). For comparison, the same Cr-spinels from different occurrences of Figure 2 are also plotted, with the exception of some spinels from the Al-bearing augite dikes used for heating stages (Menegazzo et al. 1997).

DISCUSSION AND CONCLUSIONS

Princivalle et al. (1989) argued that within a single suite of mantle xenoliths, the ratio of the M-O to T-O bond lengths, and consequently u , are constant, despite important changes in composition. Conversely, u may differ in suites with similar bulk-composition but different degrees of Mg-Al order between T and M sites. This pattern is related to the physical environment as, for example, the cooling history experienced by the rocks. The intracrystalline Mg-Al distribution between T and M

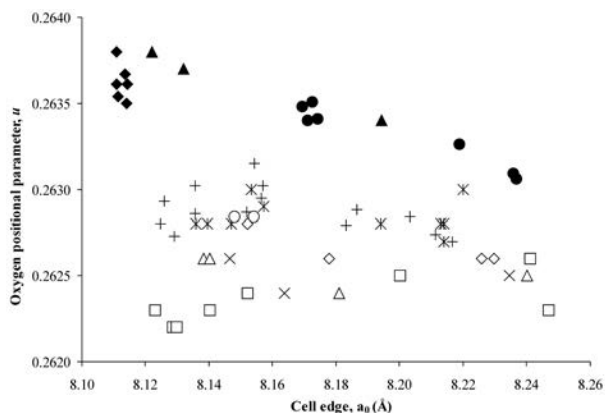


FIGURE 2. Oxygen positional parameter, u vs. cell edge, a_0 (Å). Full circles: this study; full triangle: Balmuccia mantle peridotite and transitional dikes (Basso et al. 1984; Princivalle et al. 1989); full diamonds: Balmuccia Al-dikes (Basso et al. 1984; Menegazzo et al. 1997); open squares: Mt. Leura (Della Giusta et al. 1986); open triangles: NE Brazil (Princivalle et al. 1989); open diamonds: Assab (Princivalle et al. 1989); crosses: Mt. Noorat (Princivalle et al. 1989); asterisks: Predazzo (Carraro 2003); plus: San Carlos (Uchida et al. 2005); open circles: Hungary (Nédlí et al. 2008).

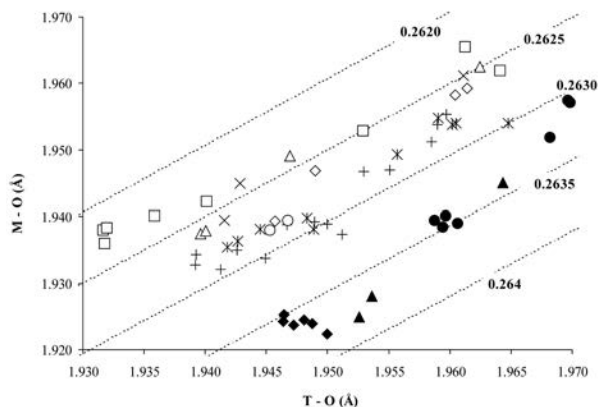


FIGURE 3. M-O vs. T-O bond lengths. Symbols as in Figure 2. Dotted lines represent equal u values.

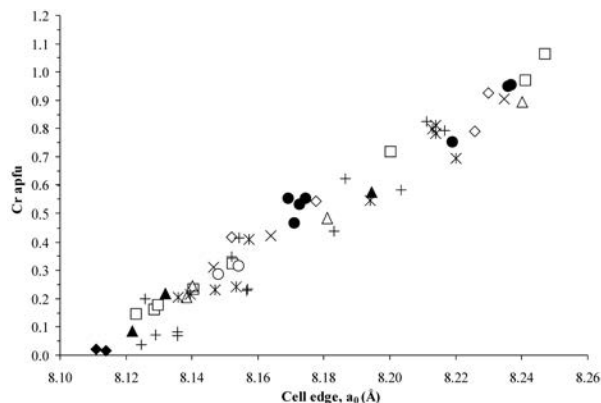


FIGURE 4. Cr (apfu) vs. cell edge, a_0 (Å). Symbols as in Figure 2.

sites of natural spinels mainly depends on the thermal history of the host rocks. The dependence of cation distributions on temperature has been investigated by several studies (O'Neill and Navrotsky 1983, 1984; Della Giusta and Ottonello 1993; Nell and Wood 1991; Della Giusta et al. 1996; Princivalle et al. 1999; Lucchesi et al. 2010). When the cooling path is very slow, Mg and Al cations strongly order in T and M sites, respectively, whereas fast quenching preserves disordered cation distribution (Princivalle et al. 1989; Della Giusta et al. 1996; Lucchesi and Della Giusta 1997).

Figures 2 and 3 show how Cr-spinels from lherzolite mantle xenoliths always present u values lower than those of Cr-spinels from lherzolite in mantle peridotites. In our samples, cooling was very slow as suggested by the ordered distribution of Mg(M) and Al(T) (inversion parameter below 0.08), respectively (Table 1). Moreover, the cooling rate of mantle peridotite seems to be slower than that of mantle xenoliths, given that the u values are higher.

Obata (1980) proposed that the mineralogical zonation developed through a recrystallization of a hot (1100 to 1200 °C) solid mantle peridotite during its ascent into the Earth's crust. According to Van der Wal and Vissers (1993), the spinel tectonites in the northwestern part of Ronda massif constitute a fairly homogeneous zone of foliated lherzolites, the core of orthopyroxene clasts suggesting temperatures at about 1110 ± 65 °C at spinel-peridotite facies conditions, whereas the mineral chemistry of the pyroxene neoblasts suggest recrystallization at lower temperatures (811–896 °C), consistent with progressive cooling during the development of the spinel tectonites. Lenoir et al. (2001) suggested that there was a smooth thermal gradient across the Ronda massif and that preservation of the spinel tectonites and mylonites in the upper part of the body is a result of the transient nature of the thermal event. They suggested that the pyroxene compositions were not fully re-equilibrated during this event. Based on additional pyroxene thermobarometry, they calculated that conditions on the recrystallization front within the massif, where the spinel tectonites become modified by grain growth and melt percolation, were around 1180–1225 °C (Fig. 5). For Ronda and Beni Bousera (Morocco) massifs, Woodland et al. (2006) determined the equilibration temperatures using the two-pyroxene thermometer of Brey and Köhler (1990) and an

assumed pressure of 9 kbar (Woodland et al. 1992). Calculated temperatures range from 833 to 1137 °C (Fig. 5). Applications of the olivine-spinel thermometer of Li et al. (1995) yielded a similar range in temperatures from 840 to 1005 °C (Fig. 5) where the samples recording lower temperature are from the Ronda massif.

By using the thermometer for the calculation of intracrystalline closure temperature by Princivalle et al. (1999), temperatures between 640 and 680 °C for the spinels with low-Cr content, and between 740 and 840 °C for those having higher Cr content, have been determined. The higher temperatures are very close to the intercrystalline temperatures based on the olivine-spinel thermometer by Li et al. (1995) calculated by Woodland et al. (2006).

It should be noted that the lower u values are also related to the higher a_0 values (Fig. 2). As we already stated, a_0 is related to Cr content (Fig. 4). In Figure 6, there is a linear relationship between u and Cr content for samples from mantle peridotites (Ronda and Balmuccia) but not for mantle xenoliths. The u value in Cr-spinels different from those in mantle xenoliths seems to be driven solely by the chemistry of the spinels. Moreover, the oxygen positional parameter can be linearly related to the intracrystalline temperature for both mantle peridotite and mantle xenolith Cr-spinels (Fig. 7), whereas those from mantle xenoliths show temperatures in the range 700–1000 °C. The intracrystalline closure temperature seems to be reached faster for Cr-spinels in mantle xenoliths and is usually higher than that of Cr-spinels in mantle peridotite and associated dikes [this study and Basso et al. (1984)]. Slow crystallization temperatures in Ronda mantle peridotites are also confirmed by exsolution lamellae in pyroxenes similar to those found in Balmuccia peridotite (Basso et al. 1984).

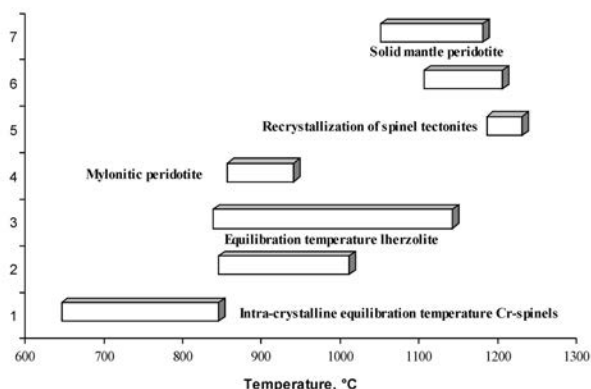


FIGURE 5. Temperatures within the Ronda massif. 1 = intracrystalline equilibration temperature of Cr-spinels (this study); 2 = olivine-spinel equilibration temperature in lherzolite (Ronda and Rif massifs; Woodland et al. 2006); 3 = two-pyroxene equilibration temperature in lherzolite (Ronda and Rif massifs; Woodland et al. 2006); 4 = two-pyroxene, Ca and Al in orthopyroxene thermometers (Van der Wal and Vissers 1993); 5 = two-pyroxene thermometer for spinel tectonites (Lenoir et al. 2001); 6 = two-pyroxene, olivine-spinel and Al in orthopyroxene thermometers (Obata 1980). 7 = two-pyroxene, Ca and Al in orthopyroxene thermometers (Van der Wal and Vissers 1993). Explanations are in the text.

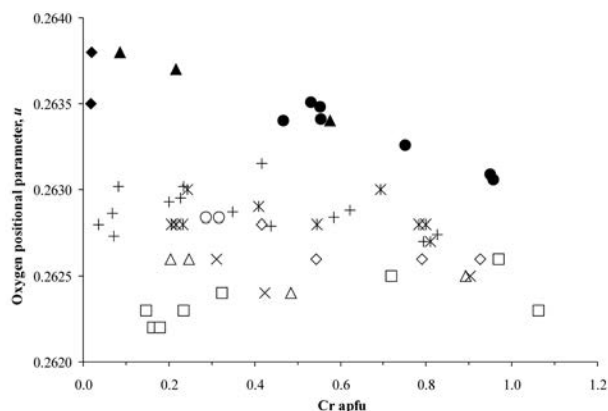


FIGURE 6. Oxygen positional parameter, u vs. Cr (apfu). Symbols as in Figure 2.

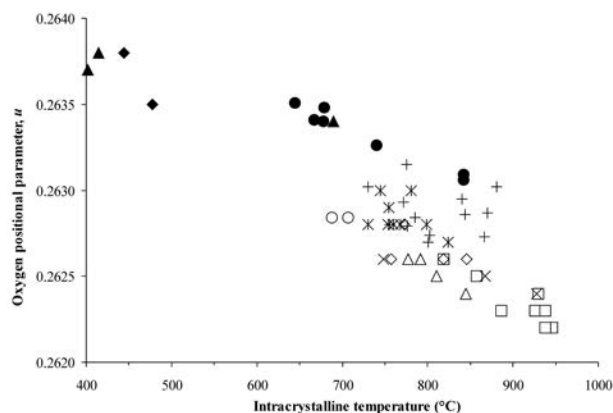


FIGURE 7. Oxygen positional parameter, u vs. intracrystalline temperature (°C) of Cr-spinels. Symbols as in Figure 2.

ACKNOWLEDGMENTS

The Italian C.N.R. financed the installation and maintenance of the microprobe laboratory in Padova. R. Carampin, L. Tauro, and L. Furlan are kindly acknowledged for technical support. This work was supported with MURST and Trieste University grants to F.P. (Studio dello stato di ossidazione e degli elementi in tracce in spinelli a Fe e Cr: implicazioni petrologiche. PRIN 2008). A. Della Giusta, F. Bosi, and R. Peterson are kindly thanked for their valuable comments.

REFERENCES CITED

- Barnes, S.J. and Roeder, P.L. (2001) The range of spinel compositions in terrestrial mafic and ultramafic rocks. *Journal of Petrology*, 42, 2279–2302.
- Basso, R., Comin-Chiaramonti, P., Della Giusta, A., and Flora, O. (1984) Crystal chemistry of four Mg-Fe-Al-Cr spinels from the Balmuccia peridotite (Western Italian Alps). *Neues Jahrbuch für Mineralogie Abhandlungen*, 150, 1–10.
- Booth-Rea, G., Azañón, J.M., Martínez-Martínez, J.M., Vidal, O., and García Dueñas, V. (2005) Contrasting structural and P-T evolution of tectonic units in the southeastern Betics: Key for understanding the exhumation of the Alboran Domain HP/LT crustal rocks (western Mediterranean). *Tectonics*, 24, 1–24.
- Bosi, F., Andreozzi, G.B., Ferrini, V., and Lucchesi, S. (2004) Behavior of cation vacancy in kenotetrahedral Cr-spinels from Albanian eastern belt ophiolites. *American Mineralogist*, 89, 1367–1373.
- Brey, G.P. and Köhler, T. (1990) Geothermometry in four-phase lherzolites: II. New thermobarometers and practical assessment of existing thermobarometers. *Journal of Petrology*, 31, 1353–1378.
- Carbonin, S., Russo, U., and Della Giusta, A. (1996) Cation distribution in some natural spinels from X-ray diffraction and Mössbauer spectroscopy. *Mineralogical Magazine*, 60, 355–368.
- Carraro, A. (2003) Crystal chemistry of chromian spinels from a suite of spinel peridotite mantle xenoliths from the Predazzo Area (Dolomites, Northern

- Italy). *European Journal of Mineralogy*, 15, 681–688.
- Della Giusta, A. and Ottonello, G. (1993) Energy and long-range disorder in simple spinels. *Physics and Chemistry of Minerals*, 20, 228–241.
- Della Giusta, A., Princivalle, F., and Carbonin, S. (1986) Crystal chemistry of a suite of natural Cr-bearing spinels with $0.15 < Cr < 1.07$. *Neues Jahrbuch für Mineralogie Abhandlungen*, 155, 319–330.
- Della Giusta, A., Carbonin, S., and Ottonello, G. (1996) Temperature-dependant disorder in a natural Mg-Al-Fe²⁺-Fe³⁺-spinel. *Mineralogical Magazine*, 60, 603–616.
- Dick, H.J.B. and Bullen, T. (1984) Chromian spinel as a petrogenetic indicator in abyssal and alpine-type peridotites and spatially associated lavas. *Contributions to Mineralogy and Petrology*, 86, 54–76.
- Esteban, J.J., Cuevas, J., Tubia J.M., Liati, A., Seward, D., and Gebauer, D. (2007) Timing and origin of zircon-bearing chlorite schists in the Ronda peridotites (Betic Cordilleras, Southern Spain). *Lithos*, 99, 121–135.
- Garrido, C.J. and Bodinier, J.L. (1999) Diversity of mafic rocks in the Ronda peridotite: Evidence for pervasive melt-rock reaction during heating of subcontinental lithosphere by upwelling asthenosphere. *Journal of Petrology*, 40, 729–754.
- Irvine, T.N. (1967) Chromian spinel as a petrogenetic indicator. Part 2. Petrologic applications. *Canadian Journal of Earth Sciences*, 4, 71–103.
- Lavina, B., Salviulo, G., and Della Giusta, A. (2002) Cation distribution and structure modeling of spinel solid solutions. *Physics and Chemistry of Minerals*, 29, 10–18.
- Lenaz, D. and Princivalle, F. (1996) Crystal-chemistry of detrital chromites in sandstones from Trieste (NE Italy). *Neues Jahrbuch für Mineralogie Monatshefte*, 429–434.
- (2005) The crystal chemistry of detrital chromian spinel from the South-eastern Alps and Outer Dinarides: The discrimination of supplies from areas of similar tectonic setting? *Canadian Mineralogist*, 43, 1305–1314.
- Lenaz, D., Andreozzi, G.B., Mitra, S., Bidyananda, M., and Princivalle, F. (2004) Crystal chemical and ⁵⁷Fe Mössbauer study of chromite from the Nuggihalli schist belt (India). *Mineralogy and Petrology*, 80, 45–57.
- Lenaz, D., Braidotti, R., Princivalle, F., Garuti, G., and Zaccarini, F. (2007) Crystal chemistry and structural refinement of chromites from different chromitite layers and xenoliths of the Bushveld Complex. *European Journal of Mineralogy*, 19, 599–609.
- Lenaz, D., Logvinova, A.M., Princivalle, F., and Sobolev, N.V. (2009) Structural parameters of chromite included in diamonds and kimberlites from Siberia: A new tool for discriminating ultramafic source. *American Mineralogist*, 94, 1067–1070.
- Lenoir, H., Garrido, C.J., Bodinier, J.-L., Dautria, J.-M., and Gervilla, F. (2001) The recrystallization front of the Ronda peridotite: Evidence for melting and thermal erosion of subcontinental lithospheric mantle beneath the Alboran Basin. *Journal of Petrology*, 42, 141–158.
- Li, J.-P., Kornprobst, J., and Vielzeuf, D. (1995) An improved experimental calibration of the olivine-spinel geothermobarometer. *Chinese Journal of Geochemistry*, 14, 68–77.
- Lucchesi, S. and Della Giusta, A. (1997) Crystal chemistry of a highly disordered Mg-Al natural spinel. *Mineralogy and Petrology*, 59, 91–99.
- Lucchesi, S., Bosi, F., and Pozzuoli, A. (2010) Geothermometric study of Mg-rich spinels from the Somma-Vesuvius volcanic complex (Naples, Italy). *American Mineralogist*, 95, 617–621.
- Menegazzo, G., Carbonin, S., and Della Giusta, A. (1997) Cation and vacancy distribution in an artificially oxidized natural spinel. *Mineralogical Magazine*, 61, 411–421.
- Nédli, Zs., Princivalle, F., Lenaz, D., and Tóth, T.M. (2008) Crystal chemistry of clinopyroxene and spinel from mantle xenoliths hosted in Late Mesozoic lamprophyres (Villány Mts., South Hungary). *Neues Jahrbuch für Mineralogie Abhandlungen*, 185, 1–10.
- Nell, J. and Wood, B.J. (1991) High-temperature electrical measurements and thermodynamic properties of Fe₃O₄-FeCr₂O₄-MgCr₂O₄-FeAl₂O₄ spinels. *American Mineralogist*, 76, 405–426.
- North, A.C.T., Phillips, D.C., and Scott-Mattews, F. (1968) A semi-empirical method of absorption correction. *Acta Crystallographica*, A24, 351–352.
- Obata, M. (1980) The Ronda peridotite gamet-lherzolite, spinel-lherzolite, and plagioclase-lherzolite facies and the P-T trajectories of a high-temperature mantle intrusion. *Journal of Petrology*, 21, 533–572.
- O'Neill, H.St.C. and Navrotsky, A. (1983) Simple spinels: crystallographic parameters, cation radii, lattice energies and cation distributions. *American Mineralogist*, 68, 181–194.
- (1984) Cation distributions and thermodynamic properties of binary spinel solid solutions. *American Mineralogist*, 69, 733–753.
- Platt, J.P., Argles, T.W., Carter, A., Kelley, S.P., Whitehouse, M.J., and Lonergan, L. (2003) Exhumation of the Ronda peridotite and its crustal envelope: constraints from thermal modeling of a P-T-time array. *Journal of the Geological Society*, 160, 655–676.
- Platt, J.P., Anczkiewicz, R., Soto, J.-I., Kelley, S.P., and Thirlwall, M. (2006) Early Miocene continental subduction and rapid exhumation in the western Mediterranean. *Geology*, 34, 981–984.
- Preçigout, J., Gueydan, F., Gapais, D., Garrido, C.J., and Essaifi, A. (2007) Strain localisation in the subcontinental mantle: A ductile alternative to the brittle mantle. *Tectonophysics*, 445, 318–336.
- Prince, E. (2004) *International Tables for X-ray Crystallography. Volume C: Mathematical, Physical and Chemical Tables*, 3rd ed. Springer, Dordrecht, The Netherlands.
- Princivalle, F., Della Giusta, A., and Carbonin, S. (1989) Comparative crystal chemistry of spinels from some suits of ultramafic rocks. *Mineralogy and Petrology*, 40, 117–126.
- Princivalle, F., Della Giusta, A., De Min, A., and Piccirillo, E.M. (1999) Crystal chemistry and significance of cation ordering in Mg-Al rich spinels from high grade hornfels (Predazzo-Monzoni, NE Italy). *Mineralogical Magazine*, 63, 257–262.
- Quintiliani, M., Andreozzi, G.B., and Graziani, G. (2006) Fe²⁺ and Fe³⁺ quantification of different approaches and f_{o2} estimation for Albanian Cr-spinels. *American Mineralogist*, 91, 907–916.
- Reisberg, L. and Lorand, J.P. (1995) Longevity of sub-continental mantle lithosphere from osmium isotope systematics in orogenic peridotite massifs. *Nature*, 376, 159–162.
- Roeder, P.L. (1994) Chromite: from the fiery rain of chondrules to the Kilauea Iki lava lake. *Canadian Mineralogist*, 32, 729–746.
- Sack, R.O. (1982) Spinel as petrogenetic indicators: Activity-composition relations at low pressures. *Contributions to Mineralogy and Petrology*, 79, 169–186.
- Sack, R.O. and Ghiorso, M.S. (1991) Chromian spinels as petrogenetic indicators: Thermodynamics and petrological applications. *American Mineralogist*, 76, 827–847.
- Sheldrick, G.M. (1997) SHELX-97-1. Program for crystal structure refinement. University of Göttingen, Germany.
- Sinigoï, S., Comin-Chiaromonti, P., Demarchi, G., and Siena, F. (1983) Flow differentiation in the mantle: evidence from the Balmuccia peridotite (Ivrea-Verbano zone, Western Alps, Italy). *Contributions to Mineralogy and Petrology*, 82, 351–359.
- Tokonami, M. (1965) Atomic scattering factor for O²⁻. *Acta Crystallographica*, 19, 486.
- Tubia, J.M., Cuevas, J., and Gil Ibarra, J.I. (1997) Sequential development of the metamorphic aureole beneath the Ronda peridotites and its bearing on the tectonic evolution of the Betic Cordillera. *Tectonophysics*, 279, 227–252.
- Uchida, H., Lavina, B., Downes, R.T., and Chesley, J. (2005) Single-crystal X-ray diffraction of spinels from the San Carlos Volcanic Field, Arizona: Spinel as a geothermometer. *American Mineralogist*, 90, 1900–1908.
- Van der Wal, D. and Bodinier, J.L. (1996) Origin of the recrystallisation front in the Ronda peridotite by km-scale pervasive porous melt flow. *Contributions to Mineralogy and Petrology*, 122, 387–405.
- Van der Wal, D. and Vissers, R.L.M. (1993) Uplift and emplacement of upper-mantle rocks in the Western Mediterranean. *Geology*, 21, 1119–1122.
- (1996) Structural petrology of the Ronda peridotite, SW Spain: Deformation history. *Journal of Petrology*, 37, 23–43.
- Woodland, A.B., Kornprobst, J., and Wood, B.J. (1992) Oxygen thermobarometry of orogenic lherzolite massifs. *Journal of Petrology*, 33, 203–230.
- Woodland, A.B., Kornprobst, J., and Tabit, A. (2006) Ferric iron in orogenic lherzolite massifs and controls of oxygen fugacity in the upper mantle. *Lithos*, 89, 222–241.

MANUSCRIPT RECEIVED MARCH 4, 2010

MANUSCRIPT ACCEPTED MAY 2, 2010

MANUSCRIPT HANDLED BY G. DIEGO GATTA